Anomalous edge states and topological phases of a kicked quantum Hall system

Mahmoud Lababidi, Indubala I. Satija, and Erhai Zhao
School of Physics, Astronomy, and Computational Sciences, George Mason University, Fairfax, VA 22030

Periodically driven quantum Hall system at a fixed flux is found to exhibit a series of phases featuring anomalous edge modes with the "wrong" chirality. This leads to pairs of counter-propagating chiral edge modes at each edge, in sharp contrast to stationary quantum Hall systems. We show that these anomalous edge modes are robust against weak disorder. They are essential in distinguishing phases with the same Chern and winding numbers. Their existence thus challenges the existing framework describing the topological properties of driven systems. We explore their origin using a simplified model and discuss their experimental signatures.

PACS numbers:

Cyclic time-evolutions of quantum systems are known to have interesting topological properties [1, 2]. Several groups recently showed that periodic driving can turn an ordinary band insulator (superconductor) into a Floquet topological insulator (superconductor) [3–10]. This provides a powerful way to engineer effective Hamiltonians that stroboscopically mimic stationary topological insulators [4, 5]. Moreover, a large class of topological phenomena in periodically driven many-body systems are unique and have no stationary counterparts. An early example is Thouless's one-dimensional charge pump, where he showed that the charge transport is quantized and related to a topological invariant [11]. Other topological invariants for the time evolution operator in two and three dimensions have been constructed recently [3, 5, 10]. Yet a systematic classification of these invariants analogous to the periodic table of symmetry protected topological phases [12, 13] is still to be achieved.

In this paper, we identify new topological phenomena in a lattice integer quantum Hall (QH) system under cyclic driving with period T. For fixed magnetic flux, variations of the driving parameter induce topological phase transitions where the Chern numbers of the quasienergy bands change. We find multiple phases of the driven QH system featuring counter-propagating chiral edge modes at the each edge, and show they are robust against disorder. In particular, there appear "π-modes", pairs of edge modes with opposite chirality at quasienergy π/T. These anomalous edge modes differ from those found previously in other driven two-dimensional (2D) lattice models, where the edge modes at quasienergy π/T all propagate in the same direction and subsequently their number can be inferred either from the Chern number or the winding number [5, 10]. Here, these known topological invariants can not predict the number of edge modes of each chirality, but only their difference. For example, we find two phases (phase B and D below) having the same set of Chern and winding numbers but very different edge state spectra. New theoretical framework is needed to fully characterize and understand the the topological properties of such deceivingly simple systems.

Our work is motivated by recent experimental achievements of artificial magnetic field for ultracold atoms [14, 15] and temporal modulation of optical lattices [16, 17]. We consider a model consisting of (spinless) fermionic atoms loaded onto a square optical lattice. Each site is labeled by vector $\mathbf{r} = n\hat{x} + m\hat{y}$, where n, m are integers, $\hat{x}$ ($\hat{y}$) is the unit vector in the x (y) direction, and the lattice spacing a is set to be the length unit. The tight binding Hamiltonian has the form

$$H = -J_x \sum_{\mathbf{r}} |\mathbf{r}+\hat{x}\rangle\langle\mathbf{r}| - J_y \sum_{\mathbf{r}} |\mathbf{r}+\hat{y}\rangle e^{i2\pi n\alpha}\langle\mathbf{r}| + h.c. \quad (1)$$

Here, $|\mathbf{r}\rangle$ is the Wannier state localized at site $\mathbf{r}$. J_x (J_y) is the nearest neighbor hopping along the x (y) direction. We assume a uniform synthetic magnetic field B is applied in the $-z$ direction, and work in the Landau gauge, $A_x = 0$, $A_y = -Bx$. The flux per plaquette, in units of the flux quantum Φ_0, is $\alpha = -Ba^2/\Phi_0$. Field B gives rise to the Peierls phase factor $e^{i2\pi n\alpha}$ in the hopping. For static J_x, J_y, H is the well known Hofstadter model [20].

We investigate a class of periodically driven quantum Hall systems described by H above, but with J_x and J_y being periodic functions of time t. We will focusing on the following driving protocol

$$\begin{aligned} &J_x(t) = J_x, \quad J_y(t) = 0. \quad 0 < \mathrm{mod}(t,T) < \tau \\ &J_x(t) = 0, \quad J_y(t) = J_y. \quad \tau < \mathrm{mod}(t,T) < T \end{aligned} \quad (2)$$

Namely, within one period T, the hopping along x is turned on during the interval $(0,\tau)$, while the hopping along y is turned on during the interval (τ,T).We then have two independent driving parameters,

$$\theta_x = J_x\tau/\hbar, \quad \theta_y = J_y(T-\tau)/\hbar.$$

While it is hard to achieve in solid state systems, temporal modulation of J_x or J_y is straightforward to implement for cold atoms in optical lattices, e.g., by simply tuning the intensity of the laser. In the limit $\tau \to T$ and $(T-\tau)J_y \to$const, the driving protocol becomes

$$J_x(t) = J_x, \quad J_y(t) = J_y T \sum_j \delta(t - jT), \quad (3)$$

i.e., the y hopping is only turned on when $t = jT$, with j any integer. In this limit, $\theta_x = J_x T/\hbar$, $\theta_y = J_y T/\hbar$. We will simplify refer to systems described by (2) or (3) as kicked quantum Hall systems, because (3) resembles the well studied kicked rotors.

The time evolution operator of the system, defined by $|\psi(t)\rangle = U(t)|\psi(0)\rangle$, has the formal solution $U(t) = \mathcal{T}\exp[-i\int_0^t H(t')dt']$, where $\mathcal{T}$ denotes time-ordering and we set $\hbar = 1$ throughout. The discrete translation symmetry $H(t) = H(t+T)$ leads to a convenient basis $\{|\phi_\ell\rangle\}$, defined as the eigenmodes of Floquet operator $U(T)$,

$$U(T)|\phi_\ell\rangle = e^{-i\omega_\ell T}|\phi_\ell\rangle.$$

Here the quasienergy ω_ℓ, by definition, is equivalent to $\omega_\ell + 2p\pi/T$ for any integer p and lives within the quasienergy Brillouin zone (QBZ), $\omega \in [-\pi/T, \pi/T)$. For rational flux $\alpha = 1/q$, U is a $q \times q$ matrix in momentum space and there are q quasienergy bands. For convenience, we label the lowest band within the QBZ with $\ell = 1$, and the subsequent bands at increasingly higher quasienergies with $\ell = 2, 3, ..., q$. Correspondingly, we call the gap below the ℓ-th band the ℓ-th gap. For example, the gap around $\pm\pi/T$ is the first gap. The Chern number for the ℓ-th quasienergy band can be defined analogous to the stationary case [21]

$$c_\ell = \frac{i}{2\pi}\int dk_x dk_y \left[\partial_{k_x}\phi_\ell^*(\mathbf{k})\partial_{k_y}\phi_\ell(\mathbf{k}) - c.c.\right],$$

where the integration is over the magnetic Brillouin zone, and $\phi_\ell(\mathbf{k})$ is the ℓ-th eigenwavefunction of $U(\mathbf{k}, T)$.

Figure 1 displays four representative quasienergy spectra of a finite slab of length L in the x direction under periodic driving (2). As in static QH systems, we observe edge states forming within the quasienergy gaps. Consider the left edge ($x = 0$) and let us denote the number of chiral edge modes propagating in the $\hat{y}$ ($-\hat{y}$) direction by n_ℓ^+ (n_ℓ^-). For driven 2D systems, the Chern numbers are generally insufficient to predict (n_ℓ^+, n_ℓ^-). Instead, as shown by Rudner et al [10], the net chirality of the edge modes inside the ℓ-th quasienergy gap, $w_\ell \equiv n_\ell^+ - n_\ell^-$, is given by the following winding number

$$w_\ell = \int \frac{dk_x dk_y dt}{24\pi^2}\epsilon^{\mu\nu\rho}\mathrm{Tr}\left[(u^{-1}\partial_\mu u)(u^{-1}\partial_\nu u)(u^{-1}\partial_\rho u)\right].$$

Here $\mu, \nu, \rho = 1, 2, 3$ corresponds to k_x, k_y, t respectively, and $u(\mathbf{k}, t)$ is a smooth extrapolation of $U(\mathbf{k}, t)$ [10]

$$u(\mathbf{k}, t) = U(\mathbf{k}, 2t)\theta(T/2 - t) + e^{-i\mathscr{H}(\mathbf{k})2(T-\tau)}\theta(t - T/2),$$

where $\mathscr{H}(\mathbf{k}) = -(i/T)\log U(T)$ is the effective Hamiltonian with the branch cut of the logarithm chosen at quasienergies within the ℓ-th gap. In fact, as shown in Ref. [10], the Chern numbers can be inferred from the winding numbers by the relation $c_\ell = w_{\ell+1} - w_\ell$.

Applying the theoretical analysis outlined above, we obtain Fig. 2, the zero temperature "phase diagram"

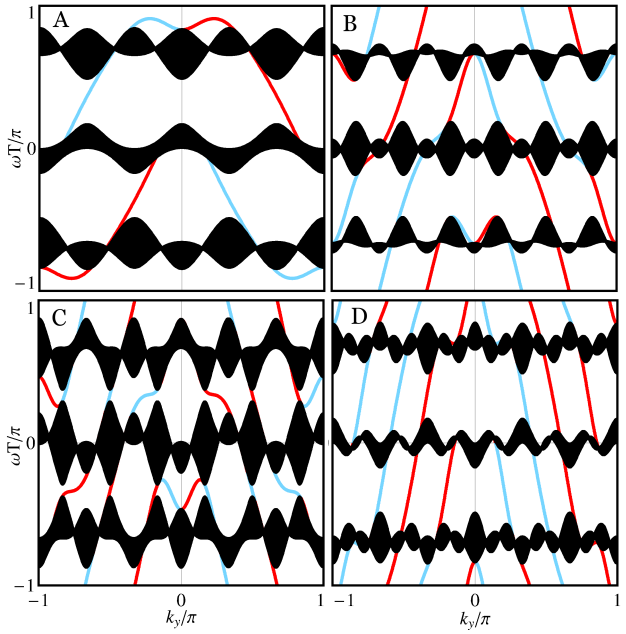

FIG. 1: (color online) Quasienergy spectra of a finite (in the x-direction) slab of periodically driven quantum Hall system at flux $-1/3$ and fixed $\theta_x = \pi/3$. The four panels, $\theta_y = 0.5\pi$, π, 1.2π, and 1.5π, correspond to phase A, B, C, and D, respectively, shown in Fig. 2. Edge states localized on the left (right) edge are shown in blue (red).

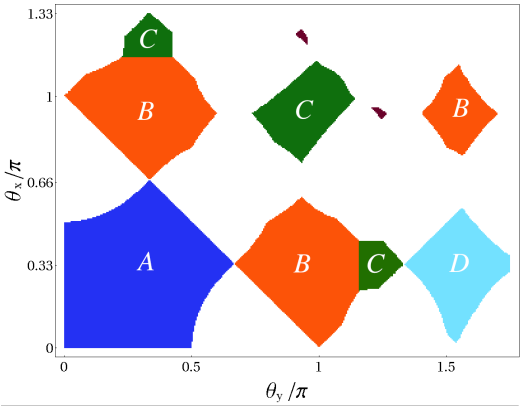

	A	B	C	D
(n_1^+, n_1^-)	(0,0)	(1,1)	(1,1)	(2,2)
(n_2^+, n_2^-)	(0,1)	(2,0)	(0,4)	(1,2)
(n_3^+, n_3^-)	(1,0)	(0,2)	(4,0)	(2,1)
w_1, w_2, w_3	0,-1,1	0,2,-2	0,-4,4	0,-1,1
c_1, c_2, c_3	-1,2,-1	2,-4,2	-4,8,-4	-1,2,-1

FIG. 2: (color online) Phase diagram of a periodically driven quantum Hall system in the plane spanned by driving parameter θ_x and θ_y at flux $\alpha = -1/3$. Each phase (A, B, C, and D) is characterized by $\{(n_\ell^+, n_\ell^-)\}$, the number of modes within the ℓ-th gap and propagating along $\pm\hat{y}$ at the left edge. The winding number of the ℓ-th gap $w_\ell = n_\ell^+ - n_\ell^-$, and the Chern number of the ℓ-th band $c_\ell = w_{\ell+1} - w_\ell$ (see main text).

of the kicked quantum Hall system in terms of two independent driving parameters, θ_x and θ_y. It showcases four representative phases, labelled by A to D, for flux $\alpha = -1/3$. All of them feature three well defined quasienergy bands and three gaps, while the spectrum in the rest of the phase diagram is largely gapless. The corresponding spectrum of each phase in the slab geometry can be found in Figure 1. The table in Fig. 2 summarizes what we know about each phase: the number of edge modes on the left edge propagating in the $\pm\hat{y}$ direction, (n_ℓ^+, n_ℓ^-), inside the ℓ-th gap; the winding number w_ℓ of the ℓ-th gap; and the Chern number c_ℓ of the ℓ-th band. Note that w_ℓ and c_ℓ are calculated independently from the bulk spectrum. We also note that at the phase transition points where the gap closes, the Chern numbers always change by a multiple of 3, consistent with the Diophantine equation [18]. In what follows, we discuss in turn each of these phases.

(A). The main features of phase A can be understood by considering the fast driving limit, $\theta_1, \theta_2 \ll 1$. The effective Hamiltonian $\mathscr{H}$, takes the same form of H in Eq. (1), only with the bare hopping replaced by the effective hopping $J_x \to J_x\tau/T$, $\quad J_y \to J_y(1-\tau/T)$. The driven system in phase A stroboscopically mimics a static QH system with the same flux but renormalized hopping. In particular, there is no edge state crossing the gap centered round $\pm\pi/T$.

(B). Phase B highlights a remarkable consequence of periodic driving: there are now two chiral edge modes inside the second and third gap. This is in sharp contrast to phase A, not only in the number of edge modes, but also in their chirality. Thus, simple periodic modulations of hopping proposed here is sufficient to change both the number and the chirality of edge states. More importantly, phase B contains a pair of counter-propagating edge modes, dubbed "π-modes", inside the first gap at the QBZ boundary $\pm\pi/T$. Note that the net chirality is zero, $w_1 = n_1^+ - n_1^- = 0$. Previous work on driven 2D systems [5, 10] also found chiral edge modes at $\pm\pi/T$. However, there the π-modes all have the same chirality, and the nearby bands are trivial with zero Chern number. Then the following two questions naturally arise. What is the origin of such pairs of π-modes? Are they robust against perturbations? Counter-propagating chiral edge modes at the same edge are usually argued to be unstable, because backscattering may couple them leading to the opening of a gap. However, a closer inspection reveals that the two π-modes of opposite chirality (shown in blue for the left edge) cross the QBZ boundary at k_y^a and $k_y^b = k_y^a + \pi$ respectively, where the precise value of k_y^a depends on $\theta_{x,y}$. Thus backscattering, $k_y \to -k_y$, does not directly hybridize them. We have verified the stability of the π-modes against disorder by numerically solving for the spectra of finite systems of dimension $L_x \times L_y$ in the presence of static on-site disorder potential, $\delta\mu(\mathbf{r}) \in (-\Delta, \Delta)$. To resolve the number of edge states within the first gap, we define spectral function $\rho(k_y, \omega) = \sum_{n, x<L_x/2} \delta(\omega - E_n) |\sum_y \psi_n(x,y) e^{-ik_y y}/L_y|^2$, where the sum over x is restricted to the left half of the slab, E_n and ψ_n are the n-th quasienergy and the corresponding eigenwavefunction, respectively. As shown in Fig. 3, $\rho(k_y, \omega)$ for $\Delta = 0.3J_x$ is peaked at two different k_y values, with separated approximately by π, suggesting two edge modes near π/T. These evidences indicate that the π-modes are stable against weak disorder.

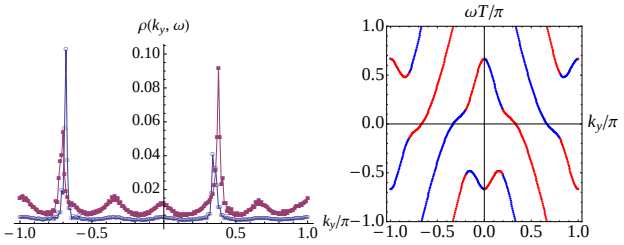

FIG. 3: (color online) Left: Robust edge states in the presence of disorder $\Delta = 0.3J_x$. The two peaks in the spectral function for $\omega = 0.95\pi/T$ (circle) and $0.85\pi/T$ (filled square) suggest two π-modes at the left edge, consistent with Fig. 1B. Right: Winding of the quasienergy spectrum of a two-leg ladder. Red (blue) indicates the eigenstate is predominantly on the right (left) leg. $\alpha = -1/3$, $\theta_x = \pi/3$, $\theta_y = \pi$.

(C) Phase C is very similar to phase B. The only difference is that there are 4 (instead of 2 in phase B) chiral edge modes propagating in the same direction inside the second and third gap. This is yet another example that Chern numbers of the quasi-energy bands can be controlled by periodic driving.

(D) Phase D is qualitatively different from all other phases. Firstly, near the QBZ boundary, there are two pairs of counter-propagating π-modes, $n_1^+ = n_1^- = 2$. Secondly, the edge states within the second and third gap also contain counter-propagating modes: two of the edge modes propagate in the same direction, but the remaining one propagates in the opposite direction. For example, $n_2^+ = 1$, $n_2^- = 2$. Although phase D has exactly the same set of $\{w_\ell\}$ and $\{c_\ell\}$ as phase A, it has counter-propagating edge modes in all three quasienergy gaps that are robust against weak disorder. The existence of phase D thus demonstrates unequivocally that neither the winding numbers or Chern numbers give a complete characterization of the driven QH system.

Below we shed more light on the anomalous edge modes, and the successive phase transitions between the phases, using a simple model which allows analytical analysis. Consider a two-leg ladder extending infinitely in the y direction. The ladder spectrum already contains all the essential features of edge states found in large systems as shown in Figure 1. For flux 1/3, the Floquet operator of the ladder is $U(k_y, T) = e^{i\theta_y[-\cos k_y + \sigma_z\sqrt{3}\sin k_y]} e^{i\theta_x\sigma_x}$, where the σ's are Pauli matrices in the orbital space. It

follows that the effective Hamiltonian of the ladder

$$\mathscr{H}(k_y)T = \theta_y \cos k_y + \boldsymbol{\sigma} \cdot \mathbf{h}(k_y),$$

with $h(k_y) = |\mathbf{h}| = \arccos[\cos\theta_x \cos(\theta_y\sqrt{3}\sin k_y)]$. Thus, the quasienergy spectrum has two bands (branches),

$$\omega_\pm(k_y)T = \theta_y \cos k_y \pm h(k_y), \pmod{2\pi}.$$

Figure 3 shows the ladder spectrum for $\theta_x = \pi/3$ and $\theta_y = \pi$ (phase B). For vanishingly small θ_y, the bands are almost flat, $\omega_\pm \simeq \pm\theta_x/T$. As θ_y is increased, the curvature and the width of both bands increase. Beyond a critical value $\theta_y \simeq 0.57\pi$, the top of the ω_+ band (and the bottom of the ω_- band) grows beyond the QBZ, and re-enters from the opposite side of the QBZ. Consequently, the number of states crossing the QBZ boundary, $n_1^+ + n_1^-$, jumps from 0 to 4, marking a transition from phase A to phase B. From this perspective, the pair of π-modes results from the winding of quasienergy across the QBZ boundary as driving in the y-direction (θ_y) is increased. Similarly, for $\theta_y > 1.33\pi$, both the top and bottom of $\omega_\pm$ exceed the QBZ, giving rise to two pairs of π-modes at each edge in phase D. When folded into the QBZ, they intrude into the second and third bulk gap, leading to the anomalous edge mode propagating in the "wrong" direction. Remarkably, the chirality of the edge modes in Fig. 1 agrees with the predictions of the ladder model in Fig. 3. That the π-modes always appear in pairs is guaranteed by a "hidden" symmetry of $U(T)$,

$$U(k_y + \pi, T) = \sigma_z U^*(k_y, T)\sigma_z.$$

Accordingly, a quasienergy eigenvalue of $U(k_y, T)$ at π/T implies another eigenvalue at $k_y + \pi$ with quasienergy $-\pi/T$ which is equivalent to π/T. Therefore the edge states can only cross $\pm\pi/T$ even number of times at k_y values differing by π [25] Such pairs of π-modes are reminiscent of, and of course fundamentally different from, the counter-propagating edge modes protected by time-reversal symmetry in quantum spin Hall effect [22].

The anomalous edge modes unique to periodically driven QH system can be detected experimentally by momentum-resolved radio-frequency spectroscopy [23], which measures the spectral function $\rho(k_y, \omega)$. Atoms occupying the π-mode at quasienergy ω absorb radio-frequency photon and undergo a vertical transition to an empty hyperfine state which can be subsequently imaged. For example, in phase B, the measured spectral function will feature peaks at $k_y^{a,b}$ and energy $E_n = (2n+1)\pi/T$. This method can also be used to observe chiral edge states within the second and third quasienergy gap. Alternatively, the edge currents can be probed by quantum quenches that convert them into density patterns [24].

The static QH system is home to the Hofstadter butterfly, with an intricate band structure whose Chern numbers are given by the Diophantine equation. Periodic driving gives rise to new effective Hamiltonians and a rich landscape of phases which not only have new Chern numbers but also anomalous edge states and demands new ways to characterize topology of exotic states of matter.

We thank Brandon Anderson, Michael Levin, Xiaopeng Li, Takuya Kitagawa, and Mark Rudner for helpful discussions. This work is supported by AFOSR, NIST, and NSF (ML and EZ). EZ also acknowledge the support from KITP through NSF PHY11-25915.

[1] M. V. Berry, Royal Society of London Proceedings Series A **392**, 45 (1984).

[2] Y. Aharonov and J. Anandan, Phys. Rev. Lett. **58**, 1593 (1987), URL http://link.aps.org/doi/10.1103/PhysRevLett.58.1593.

[3] T. Oka and H. Aoki, Phys. Rev. B **79**, 081406 (2009), URL http://link.aps.org/doi/10.1103/PhysRevB.79.081406.

[4] N. H. Lindner, G. Refael, and V. Galitski, Nature Physics **7**, 490 (2011), ISSN 1745-2473, URL http://www.nature.com/nphys/journal/v7/n6/full/nphys1926.html.

[5] T. Kitagawa, E. Berg, M. Rudner, and E. Demler, Physical Review B **82**, 235114 (2010), URL http://link.aps.org/doi/10.1103/PhysRevB.82.235114.

[6] N. H. Lindner, D. L. Bergman, G. Refael, and V. Galitski, arXiv:1111.4518 (2011), URL http://arxiv.org/abs/1111.4518.

[7] T. Kitagawa, T. Oka, A. Brataas, L. Fu, and E. Demler, Physical Review B **84**, 235108 (2011), URL http://link.aps.org/doi/10.1103/PhysRevB.84.235108.

[8] L. Jiang, T. Kitagawa, J. Alicea, A. R. Akhmerov, D. Pekker, G. Refael, J. I. Cirac, E. Demler, M. D. Lukin, and P. Zoller, Physical Review Letters **106**, 220402 (2011), URL http://link.aps.org/doi/10.1103/PhysRevLett.106.220402.

[9] Z. Gu, H. A. Fertig, D. P. Arovas, and A. Auerbach, Physical Review Letters **107**, 216601 (2011), URL http://link.aps.org/doi/10.1103/PhysRevLett.107.216601.

[10] M. S. Rudner, N. H. Lindner, E. Berg, and M. Levin, arXiv:1212.3324 (2012), URL http://arxiv.org/abs/1212.3324.

[11] D. J. Thouless, Phys. Rev. B **27**, 6083 (1983), URL http://link.aps.org/doi/10.1103/PhysRevB.27.6083.

[12] A. Kitaev, AIP Conf. Proc. **1134**, 22 (2009).

[13] A. P. Schnyder, S. Ryu, A. Furusaki, and A. W. W. Ludwig, Phys. Rev. B **78**, 195125 (2008), URL http://link.aps.org/doi/10.1103/PhysRevB.78.195125.

[14] Y. J. Lin, R. L. Compton, K. Jimenez-Garcia, J. V. Porto, and I. B. Spielman, Nature **462**, 628 (2009), URL http://dx.doi.org/10.1038/nature08609.

[15] M. Aidelsburger, M. Atala, S. Nascimbène, S. Trotzky, Y.-A. Chen, and I. Bloch, Phys. Rev. Lett. **107**, 255301 (2011), URL http://link.aps.org/doi/10.1103/PhysRevLett.107.255301.

[16] J. Struck, C. Ölschläger, M. Weinberg, P. Hauke, J. Simonet, A. Eckardt, M. Lewenstein, K. Sengstock, and P. Windpassinger, Phys. Rev. Lett. **108**,

225304 (2012), URL http://link.aps.org/doi/10.1103/PhysRevLett.108.225304.

[17] P. Hauke, O. Tieleman, A. Celi, C. Ölschläger, J. Simonet, J. Struck, M. Weinberg, P. Windpassinger, K. Sengstock, M. Lewenstein, et al., Phys. Rev. Lett. **109**, 145301 (2012), URL http://link.aps.org/doi/10.1103/PhysRevLett.109.145301.

[18] I. Dana, Y. Avron, and J. Zak, Journal of Physics C: Solid State Physics **18**, L679 (1985), URL http://stacks.iop.org/0022-3719/18/i=22/a=004.

[19] Y. Hatsugai and M. Kohmoto, Phys. Rev. B **42**, 8282 (1990), URL http://link.aps.org/doi/10.1103/PhysRevB.42.8282.

[20] D. R. Hofstadter, Physical Review B **14**, 2239 (1976), URL http://link.aps.org/doi/10.1103/PhysRevB.14.2239.

[21] D. J. Thouless, M. Kohmoto, M. P. Nightingale, and M. den Nijs, Physical Review Letters **49**, 405 (1982), URL http://link.aps.org/doi/10.1103/PhysRevLett.49.405.

[22] C. L. Kane and E. J. Mele, Phys. Rev. Lett. **95**, 226801 (2005), URL http://link.aps.org/doi/10.1103/PhysRevLett.95.226801.

[23] J. T. Stewart, J. P. Gaebler, and D. S. Jin, Nature **454**, 744 (2008), URL http://dx.doi.org/10.1038/nature07172.

[24] M. Killi and A. Paramekanti, Physical Review A **85**, 061606 (2012), URL http://link.aps.org/doi/10.1103/PhysRevA.85.061606.

[25] The argument can be generalized to slab of any size L.